# Spin Label ESR Spectroscopy of Sarcoplasmic Reticulum $Ca^{2+}$-ATPase: Accessibility of Labeling Sites and Rotational Dynamics

**Ph.D. Thesis**

**Marianna Török**

**Department of Biochemistry, Albert Szent-Györgyi Medical University, Szeged, Hungary**

**1997**

## Papers related to the subject of the Thesis

**I. Marianna Török**, Györgyi Jakab, Alajos Bérczi, László Dux, László I. Horváth (1997) Rotational Mobility of $Ca^{2+}$-ATPase of sarcoplasmic reticulum in viscous media. *Biochimica et Biophysica Acta* (in press).

**II. Marianna Török**, Kálmán Hideg, László Dux, and László I. Horváth (1997) Accessibility of protein sulfhydryl groups to nitroxyl spin labels. *Journal of Molecular Structure* (in press).

**III.** László I. Horváth, **Marianna Török**, Kálmán Hideg, and László Dux (1997) Dynamic Aspect of Molecular Recognition. *Journal of Molecular Recognition* (submitted for publication).

**IV. Marianna Török**, Györgyi Jakab, Alajos Bérczi, László Dux, László I. Horváth (1996) Hydrodynamic Mobility of $Ca^{2+}$-ATPase of sarcoplasmic reticulum in viscous solvents. *Progress in Biophysics & Molecular Biology* **65**, suppl. 1, p. 46, P-A3-26 (Abstr.).

## Other publications

**V.** Béla Török, **Marianna Török**, Mihály Bartók (1995) Temperature and Hydrogen Pressure Dependence in the Ring Opening of Methylcyclobutane over $Pt/SiO_2$ Catalyst. *Catalysis Letters* **33**, 321-330.

**VI.** George A. Olah, Béla Török, Tatyana Shamma, **Marianna Török** and G. K. Surya Prakash (1996) Solid Acid (Superacid) Catalyzed Adamantylation of Substituted Benzenes. *Catalysis Letters* **42**, 5-13.

**VII.** George. A. Olah, G. K. Surya Prakash, Béla Török and **Marianna Török** (1996) Effect of Acid/Hydrocarbon Ratio, Temperature and Contact Time on the Isobutane-Isobutylene Alkylation Catalyzed by Trifluoromethanesulfonic Acid. *Catalysis Letters* **40,** 137-142.

## Contents

**Abbreviations and textual footnotes:**

16-SASL, 16-(N-oxy-4',4'-dimethyloxazolidin-2-yl) stearic acid;

2D, two-dimensional;

3D, three-dimensional;

5-InVSL, 3-(2-methenylindane-1,3-dione)-1-oxyl-2,2,5,5-tetramethylpyrroline;

5-MSL, 3-maleimido-1-oxyl-2,2,5,5-tetramethylpyrrolidine;

6-MSL, 4-maleimido-1-oxyl-2,2,6,6-tetramethylpiperidine;

$D_{13}$-$^{15}$N-5-InVSL,$^{15}$N-substituted, perdeuterated pyrrolyl ring containing derivative of 5-InVSL;

EGTA, ethylene glycol bis(β-aminoethyl ether)-N,N,N',N'-tetraacetic acid;

EM, electron microscopy;

ESR, electron spin resonance;

MOPS, 3-(N-morpholino)propanesulfonic acid;

NEM, N-ethylmaleimide;

SR, sarcoplasmic reticulum;

STESR, saturation transfer electron spin resonance.

## 1. Summary

The rotational diffusion of $Ca^{2+}$-ATPase [$Ca^{2+}$,$Mg^{2+}$-activated ATP phosphohydrolase E.C. 3.6.1.38] was studied in native sarcoplasmic reticulum (SR) membrane by spin label ESR spectroscopy before and after increasing the viscosity of the aqueous phase with various polyols. In parallel set of experiments the relative enzymatic activity was also followed. The ATP hydrolyzing activity of the enzyme decreased differently on adding sucrose and glycerol into the suspending medium. In the case of sucrose the reciprocal of power dependence of viscosity was observed, whereas for glycerol an exponential decay law was obtained indicating solvent-protein interaction. On increasing the viscosity of the aqueous phase by either sucrose or glycerol, no changes were observed in the intramembranous viscosity as measured using intercalated spin labeled stearic acid (16-SASL). The effective rotational correlation time of the protein ($\tau_R$) was determined, as a mobility parameter, using STESR spectroscopy after covalent labeling of the intramembranous sulfhydryl groups with N-nitroxyl derivatives of maleimide (5-MSL, 6-MSL) or an $\alpha,\beta$-unsaturated ketone (5-InVSL, $D_{13}$-$^{15}$N-5-InVSL). $\tau_R$ increased linearly with the viscosity of the sucrose containing medium and for the extramembranous size a height of 6.8 nm was obtained, indicating that approximately 82% of the volume of $Ca^{2+}$-ATPase protein is external to the sarcoplasmic reticulum. The addition of glycerol probably promoted protein-protein interaction, as indicated by the larger changes in rotational diffusion and non-linear viscosity dependence.

5-InVSL proved to be an effective nitroxyl spin label of biological macromolecules, attached rigidly due to its bulky planar side group and anchoring capability of the oxo groups to protein via hydrogen bondings. Comparing the $Ca^{2+}$-ATPase, as an integral membrane protein, and the water soluble hemoglobin several notable differences were observed in the labeling processes. In hemoglobin the sole sulfhydryl group ($\beta$93), is in a compact nonpolar structure of the protein interior and so the bulk 5-InVSL molecule has limited access to the labeling site and, hence label binding is less complete and label release (retro-Michael reaction) will be dominant. Whereas labeling sites of $Ca^{2+}$-ATPase are located in a less compact intramemranous region and so the geometrical constraint for the same spin label is not so critical offering thereby more complete access and binding. As a consequence,

paramagnetic quenching was proposed for the calibration of STESR spectral parameters using reference spectra of 5-InVSL-labeled hemoglobin, to mask the signals of nitroxyls released via the retro-Michael reaction.

## 2. Introduction with Project Settings

The dynamic behaviors of the proteins are important for many aspects of their biological function. The $Ca^{2+}$-ATPase from sarcoplasmic reticulum (SR) as a member of a large family of cation pumps, has been studied for many years from this point of view. The most of these studies have paid attention to the changes of the lipid environment, which is primarily responsible for the maintenance of the structure, segmental mobility and enzymatic activity of membrane-linked proteins (*Hidalgo, 1987*). The overall molecular mobility of transmembrane proteins is driven by the intramembranous frictional torque in the viscous hydrophobic phase unless the frictional forces in the aqueous phase are significantly increased, e.g., by adding polyols to the suspending medium (*Saffman & Delbrück, 1975; Esmann et al., 1994*). The effect of increasing viscosity in the aqueous phase depends on the relative sizes of the extramembranous-to-intramembranous parts of proteins. $Ca^{2+}$-ATPase of sarcoplasmic reticulum is an appropriate representative of numerous proteins with voluminous extramembranous protrusions (*Sandermann, 1978; Dux, 1993*). Clearly, molecular size data can be determined by rotational measurements provided the addition of polyols does not introduce large-scale conformational changes in the protein (*Sousa, 1995*). The mobility of integral membrane proteins is low; typical correlation times are in the range of $10^{-6}$ to $10^{-4}$ sec. In such instant saturation transfer ESR spectroscopy (*Thomas et al., 1976; Berliner, 1979; Marsh & Horváth, 1989*) is a suitable technique for quantitative measurements of rotational mobility and, hence, hydrodynamic sizes using covalently attached nitroxyl spin labels.

The major aim of this work was to gain a better insight into the 3D–structure of SR $Ca^{2+}$-ATPase and its modulation possibilities via alternation of in a physical parameter of the extramembrane environment. Therefore, the viscosity of the aqueous phase was increased by adding sucrose or glycerol and the rotational rate of the protein was measured by STESR

spectroscopy using covalently attached spin labeled maleimide (5-MSL). In a parallel set of experiments the changes of the relative enzymatic activity were followed. The effect of polyols on the intramembranous viscosity was checked by intercalated stearic acid spin probes (16-SASL). From hydrodynamic data the size of the extramembranous domains protruding to the aqueous phase could be determined.

In addition, our goal was to optimize the conditions of spin labeling procedure. For this reason, more rigidly attached spin labels (*Esmann et al., 1993*), the 3-(2-methenylindane-1,3-dione)-1-oxyl-2,2,5,5-tetramethylpyrroline (5-InVSL) and its $^{15}$N-substituted, perdeuterated pyrrolyl ring containing derivative ($D_{13}$-$^{15}$N-5-InVSL) were used, as well. However, the observed ESR spectra always contained more or less isotropic spectral component indicates free nitroxyl molecules prior to covalent binding or after label release due to the retro-Michael reaction (*Ingold, 1969*). On the one hand, we wanted to eliminate or mask the mobile component of STESR spectra for their correct evaluation. On the other hand, we tried to use this phenomenon as an advantage, to characterize the accessibility of the labeling sites of the proteins.

## 3. Theoretical and Historical Overview

### *3.1 Structure and Function of the SR $Ca^{2+}$-ATPase*

The $Ca^{2+}$-ATPase of SR (M. W. 113 kD) is one of the most popular member of transport proteins for structural studies due to its wide abundance and importance in the regulation of muscle contraction (*Martonosi, 1992*).The sarcoplasmic reticulum of skeletal muscle cells is an intracellular membrane compartment that stores calcium in resting conditions. Following stimulation of the muscle cell, calcium is rapidly released into the cytoplasm, allowing actin-miosin interaction and muscle contraction. The $Ca^{2+}$-ATPase - the $Ca^{2+}$ pump of the SR - transports the intracellular $Ca^{2+}$ ions by hydrolysis of ATP from the cytoplasm into the lumen of the SR during the relaxation. It has a crucial role in the maintenance of the large concentration gradient between the cytoplasmic ($[Ca^{2+}]=10^{-7}$) and luminal sides ($[Ca^{2+}]=10^{-3}$) (*Martonosi, 1984*).

The molecular structure of the enzyme was determined to 2.5 nm resolution and the height of the extramembranous segment was estimated to be ~ 6.0 nm as measured by the combined application of frozen hydration EM of the intramembranous segment and negative staining EM of the extramembranous part *(Taylor et al., 1986)*. Several data suggest that, although protein monomers retain many functions of the protein dimers, which are held together by interacting extramembranous parts, the functional unit of SR calcium pump is a dimer *(Andersen, 1989)*. The connection of the neighboring extramembranous domains has a decisive role in forming protein dimers and 2D protein crystals *(Dux & Martonosi, 1983)*. According to the three-dimensional reconstruction, protein dimers are connected by peptide-bridges formed at a height of 4.2 nm above the membrane surface. In two-dimensional $E_2$ protein crystals an additional peptide-bridge was observed at the height of 1.6 nm above the interfacial surface *(Taylor et al., 1986)*. Recently, three-dimensional cryo-electron microscopy with helical reconstruction methods can extend the resolution of the structural studies to 1.4 nm for the determination of 3D-structures of the crystals from native SR, and to 0.6 nm resolution for the structure of thin, plate like crystals of detergent-solubilized $Ca^{2+}$-ATPase *(Toyoshima et al., 1993; Stokes & Green, 1990)*. Determination of the 3D-molecular structure of $Ca^{2+}$-ATPase at higher resolution would be related this structure directly to the mechanism of $Ca^{2+}$ transport.

The complete amino-acid sequence of the $Ca^{2+}$-ATPase has been determined using complementary DNA techniques *(MacLennan et al., 1985; MacLennan, 1990)*. Based on amino-acid sequence and molecular structure data of the protein a folding model was proposed illustrating calcium transport cycle by the $Ca^{2+}$-ATPase *(MacLennan et al., 1992)*. According to this model, in $E_1$ conformation of the enzyme, high affinity $Ca^{2+}$ bindings sites located near to the center of the transmembrane domain are accessible to cytoplasmic $Ca^{2+}$, but not to luminal $Ca^{2+}$. Conformational changes induced by $Ca^{2+}$-dependent phosphorylation of $Asp^{351}$ by ATP in the cytoplasmic domain lead to the other conformation of the enzyme, $E_2$. In $E_2$ conformation the high affinity $Ca^{2+}$ binding sites are disrupted, access to the sites by cytoplasmic $Ca^{2+}$ is closed off and access to the sites by luminal $Ca^{2+}$ is gained.

$Ca^{2+}$-ATPase of SR is one of the well-characterized integral membrane proteins for which a correlation has been found between molecular dynamics and enzymatic activity data

*(MacLennan et al., 1985; Martonosi & Beeler, 1983).* The rotational diffusion data can be related to the protein size using hydrodynamic theory *(Knowles & Marsh, 1991) (vide infra).* There are several spectroscopic techniques suitable for the measurements of the microsecond rotational motions of the integral membrane proteins. For example, time resolved anisotropy measurements (absorption or phosphorescence) of long-lived triplet probes, such as erythrosin or eosin, or STESR of nitroxyl radicals were found to be excellent methods for this purpose. The present work is focused on the conventional and saturation transfer ESR of $Ca^{2+}$-ATPase.

*3.2 Molecular Dynamics of Transmembrane Proteins*

The molecular structure of several membrane proteins is known as given by *Abney & Owicki,(1985),* and *Watts & de Pont, (1985).* A common feature of the known molecular structures of membrane proteins is that transmembrane proteins consist of several segments which are located in intramembranous (i.e. in the nonpolar phase) and extramembranous parts (i.e. in the polar environment). An inevitable consequence of this arrangement is that these segments are exposed to various phases of grossly different viscosities. The mobility of transmembrane proteins is governed by the intramembranous segment since the viscosity of this phase is 200-500 mPa·s *(Cherry and Godfrey, 1981)* as compared to ~1.1 mPa·s of the aqueous phase and so the intramembranous phase has a dominant role in setting rotational diffusion *(Saffman and Delbrück, 1975).* Hence, the mobility of transmembrane proteins depends primarily on the viscosity of the intramembranous (nonpolar) phase, the size of intramembranous segments, and their aggregation state.

As a rule, the molecular size of the transmembrane segment can be determined from measured rotational correlation times. Assuming a cylinder of elliptic cross-section, denoting the semi-axes by $a$ and $b$ and the height of the membrane-spanning region of the cylinder by $h_m$, the rotational diffusion coefficient can be given *(Saffman and Delbrück, 1975), (Eq. 1).*

$$D_R = (k\,T\,F) / (4\,\pi\,\eta\,a\,b\,h_m) \qquad (1)$$

Here F denotes the shape factor for elliptic cross-section *(Jähnig, 1986), (Eq. 2).*

$$F = (2\ a/b)/[1 + (a/b)^2] \quad (2)$$

For geometrical description a membrane associated principal axis system can be defined and, to good approximation, highly anisotropic rotation is considered ($D_{R\|} >> D_{R\perp}$). The rotational correlation time $\tau_{R\|}$ is related to the principal element of the diffusion tensor $D_{R\|}$ as Eq. 3.

$$\tau_{R\|}=1/6\ D_{R\|} \quad (3)$$

The long-axis rotational correlation time $\tau_{R\|}$ is related to the effective rotational correlation time $\tau_R^{eff}$ as *Eq. 4,* assuming $D_{R\perp}$ =0 *(Robinson & Dalton, 1980; Horváth et al., 1990).*

$$\tau_{R\|} = (\tau_R^{eff} \sin^2\Theta)/2 \quad (4)$$

Thus, the effective rotational correlation time, $\tau_R^{eff}$, measured by saturation transfer ESR depends on the orientation of the spin label. As the alignment of the $z$-axis of nitroxyl molecule in the membrane fixed principal axis system is altered from $\theta$=90° to 0° the sensitivity to rotations about the long-axis is canceled. In several cases the angle between the nitroxyl z-axis and the principal rotational axis of the membrane was in the range of $\theta$=0°-30° giving low orientation dependence *(Esmann et al., 1987).* Uncertainties in the orientation and stoichiometry of the spin labels relative to the protein will set a lower limit to the applicability of such measurements for oligomer/aggregation state measurements.

The viscosity of the aqueous phase is subject to substantial alterations as the composition is altered by varying the amount of water soluble proteins and various solvents. On increasing the viscosity of the aqueous phase by polyols, like for example sucrose or glycerol, the rotational mobility is reduced as a consequence of the contribution of frictional forces at the membrane/water interface and in the aqueous environment. This effect is particularly pronounced whenever the relative sizes of the intramembranous and extramembranous segments are comparable. From rotational point of view the different segments of transmembrane proteins can be treated separately and the overall effect of frictional forces in different phases of grossly varying viscosities are determined by the

vectorial sum of the torques in the various phases *(Feynman et al. 1963; Esmann et al. 1994).* The vectorial addition of torques is based on the assumption that the different polypeptide segments are rigidly connected. The structures of known transmembrane proteins consist of, in addition to rigid binding, electrostatic interactions between the intramembranous and extramembranous segments. Furthermore, to good approximation, the steric geometry of transmembrane proteins can be described with closely collinear torques and so a scalar addition can be applied. The measured long-axis rotational correlation time has two terms corresponding to the different phases *(Esmann et al. 1994),*

$$\tau_{R\parallel} = \tau_{R\parallel}^{m} + \tau_{R\parallel}^{a} = (2\,\eta_m V_m / 3\,k\,T\,F_m) + (2\,\eta_a V_a / 3k\,T\,F_a), \quad (5)$$

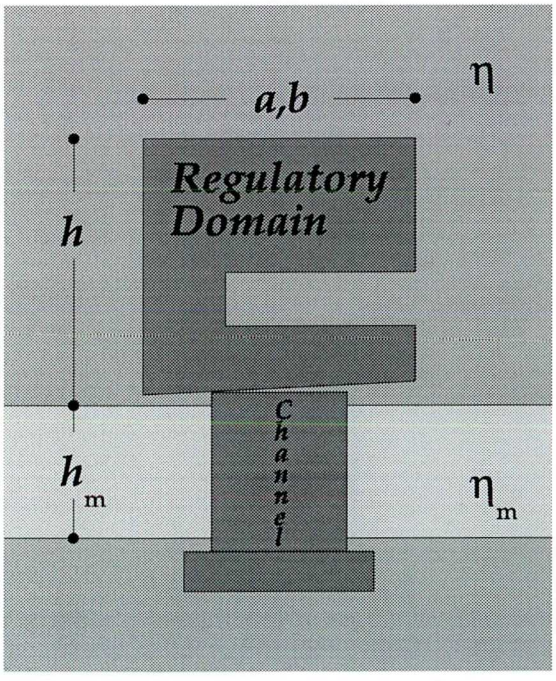


**Figure 1.** Hydrodynamic model for rotational diffusion of $Ca^{2+}$-ATPase. The central intramembranous segment is embedded in the membrane of viscosity $\eta_m$ and has a thickness of $h_m$. The two extramembranous segments which connect the loops are located in the intracellular and matrix sides in aqueous medium of viscosities $\eta_m >> \eta$, respectively. The height of the intracellular segment $h$ is indicated.

where the indices *m* and *a* refer to membranous and aqueous phases, respectively, $\tau_R^m$ and $\tau_R^a$ denote the contributions of intramembranous and extramembranous segments to the sum of the molecular rotation. Assuming that there is an evenly mobile contour across the various segments of the transmembrane protein, the shape factors *(Jähnig, 1986)* are uniform across the different segments: $F_m \approx F_a$.

For quantitative evaluation of STESR spectra of the spin labeled $Ca^{2+}$-ATPase an experimental parameter can be introduced

$$\frac{\tau_R - \tau_{R,m}}{\tau_{R,m}} = \frac{\eta V}{\eta_m V_m} \quad (6)$$

normalizing the measured correlation time increase $(\tau_R - \tau_{R,m})$ with that due to the

intramembranous contribution $\tau_{R,m}$. It should be noted that the ratio $(\tau_R - \tau_{R,m})/\tau_{R,m}$ is depending on the ratios of viscosity of the different phases ($\eta$ and $\eta_m$) and the respective volume parts of the enzyme ($V=Ah=ab\pi h$ and $V_m=A_m h_m$). The protrusion on the luminal side is neglected with respect to that on the cytosolic side ($V$) since the location of $Ca^{2+}$-ATPase in the two aqueous phases is fairly asymmetric *(MacLennan et al., 1985; Taylor et al., 1986; Toyoshima et al., 1993).* $Ca^{2+}$-ATPase, like many proteins, has a discontinuous contour at the membrane/aqueous phase interface: the areas of compact intramembranous ($A_m$) and more extensive extramembranous ($A$) segments change markedly *(Toyoshima et al., 1993; Blasie et al., 1985).* The ratio of two adjoining segments, $A/A_m$, can vary from 1, i.e. no change at the interface, to 4, corresponding to a twofold size increase. According to low-resolution diffraction measurements on two-dimensional $E_2$ crystals of $Ca^{2+}$-ATPase the ratio of the cross-sections in the extramembranous and intramembranous segments is $A/A_m \sim 3$ *(Toyoshima et al., 1993; Taylor et al., 1986; Blasie et al., 1985).* In this approximation the ratio of the extramembranous and transmembrane segments is given by

$$\frac{\tau_R - \tau_{R,m}}{\tau_{R,m}} = \frac{A}{A_m \eta_m} \eta \frac{h}{h_m} \qquad (7)$$

and so the normalized correlation time increase will be proportional to the viscosity of the aqueous phase $\eta$ and the height of the extramembranous part $h$.

*3.3 Spin Probe -Spin Label Electron Spin Resonance Spectroscopy*

Electron spin resonance is a generally applied spectroscopic method in biological systems which has a rather useful time-scale provided the relaxation rate of magnetic molecules is comparable to the rotational rate of biomolecules *(Carrington and McLachlan, 1967; Marsh and Horváth, 1989).* Spin Label ESR Spectroscopy started with design and synthesis of spin labels and apply them in biological problems similarly to the fluorescent label technique *(Ohnishi & McConnell, 1965; Stone et al., 1965, Rozantsev et al., 1971).* Several specific areas of spin labeling have been reviewed in the book "Spin labeling: Theory and Application" *(Berliner, 1976, 1979, 1989).* "Spin labels" are stable free radicals that

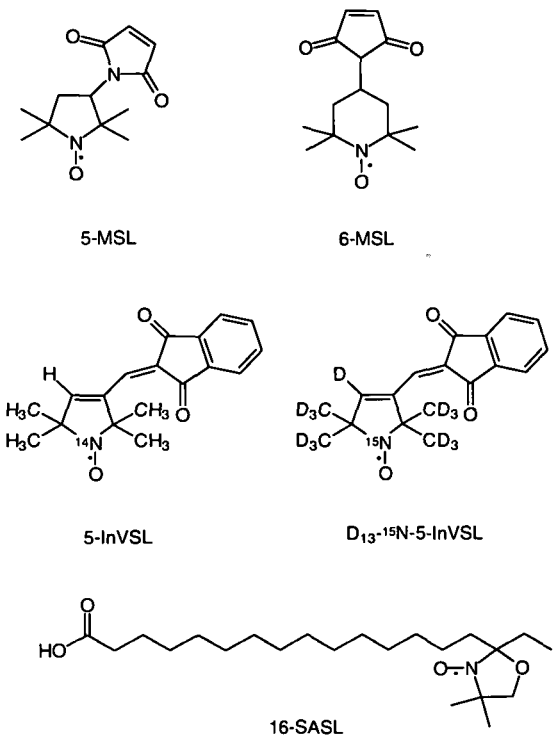


**Figure 2.** Chemical structure of spin labels and probe used in this study. One of the N-nitroxyl derivatives of maleimide (5-MSL, 6-MSL) or α,β-unsaturated ketone (5-InVSL, $D_{13}$-$^{15}$N-5-InVSL) was bound covalently to the protein for the study of its rotational motion and 16-SASL probe (stearic acid spin label) was used to monitor the hydrocarbon chain dynamics. Abbreviations are used: 5-MSL, 3-maleimido-1-oxyl-2,2,5,5-tetramethylpyrrolidine; 6-MSL, 4-maleimido-1-oxyl-2,2,6,6-tetramethylpiperidine; 5-InVSL, 3-(2-methenylindane-1,3-dione)-1-oxyl-2,2,5,5-tetramethylpyrroline; $D_{13}$-$^{15}$N-5-InVSL, $^{15}$N-substituted, perdeuterated pyrrolyl ring containing derivative of 5-InVSL; 16-SASL, 16-(N-oxy-4',4'-dimethyloxazolidin-2-yl) stearic acid.

could be attached to a specific site of a molecule in a complex system and whose ESR spectra would contain information about the environment of the label. For purposes of nomenclature, spin labels and spin probes can be distinguished. Spin labels are covalently binding free radicals by different chemical reactions (alkylation, acylation, sulfonylation, phosphorylation,...etc.). Noncovalently binding spin probes attach to the proteins by other type of interactions, such as hydrophobic, ionic or hydrogen-bonding. Nitroxyl free radicals suit the requirements of spin labels and probes, such as stability under conditions (temperature, pH, salt concentrations...etc.) used in the study of biological molecules, sensitivity to its environment (polarity, acidity, spatial restrictions, fluidity), relatively simple ESR spectra and well-understood chemistry. However, incorporating or binding of a foreign entity into a biological system it can disturb of its structure and function, which property must always be considered or minimized. "One must ensure that the reporter group is reporting the news, not making the news" *(Berliner, 1978).* Therefore chemists are making efforts to develop more appropriate reagents from this aspects *(Esmann et al., 1993).* The chemical structure of spin labels and probe, what we used in our investigations are shown in Fig. 2.

The nitroxyl radicals produce simple, well-resolved ESR spectra that are sensitive to the molecular motion and to the structure of the molecular environment. The three spectral lines of $^{14}$N ($m_I$=1) nitroxyl radicals have almost identical width and intensity for rapid

motions in low-viscosity solvents. (The spectral intensities can be proved using perdeuterated $^{15}N$ ($m_I$=1/2)-derivatives). Then the spectral lines broaden, become asymmetrical, and move increasingly further from each other with the decreasing mobility due to the size effect or increasing viscosity of media. There are three dynamic ranges in which the motional rate can quantitatively be determined by various methods of spin label ESR spectroscopy; typical spectra corresponding to these cases are shown in Fig. 3. In the case of fast tumbling rates (from $1\times10^{-11}$ to $3\times10^{-9}$ s) an essentially isotropic spectrum is observed for nitroxyl spin labels (Fig. 3A). The motional rate is characterized by the rotational correlation time which is calculated from line width measurements *(Schreier et al., 1978).* As a rule, proteins belong to the slow motion range due to size effect (from $3\times10^{-9}$ to $1\times10^{-7}$ s); the rotational correlation time of covalently attached spin labels is calculated from spectral anisotropy or line width measurements (Fig. 3B; *Freed, 1976)* Transmembrane proteins belong to the very slow motion range due to the combined effect of molecular size and large viscosity (from $1\times10^{-7}$ to $1\times10^{-3}$ s), which is evaluated from saturation experiments using a novel method (Figs. 3C and 3D), namely, saturation transfer ESR *(Thomas et al. 1976; Hyde and Dalton, 1979).*

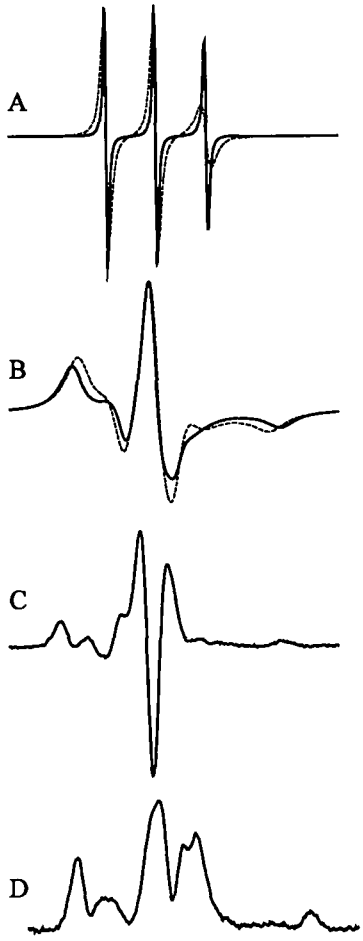


**Figure 3.** The line shape of conventional and saturation transfer electron spin resonance spectra in different time ranges between $10^{-11}$ and $10^{-3}$ s. (A) Conventional ESR of motionally averaged isotropic spectrum: $1\times10^{-10}$s (solid line) and $1\times10^{-9}$ (dashed line). (B) Conventional ESR rigid limit line shape : $5\times10^{-7}$s (solid line) and $5\times10^{-8}$s (dashed line). (C) STESR spectrum: $1\times10^{-7}$s. (D) STESR spectrum: $1\times10^{-4}$s. Total scan width is 10 mTesla

*3.4 Saturation Transfer ESR Spectroscopy*

Conventional ESR spin-label experiments may be described as "linear". At low incident microwave field intensity ($H_1$) the spectral intensities are linearly proportional to $H_1$, and there is no saturation. Saturation transfer ESR (STESR) is one of the so-called nonlinear methods, where the incident microwave field intensity is sufficient to cause a significant departure from thermal equilibrium and the observed spectral line shapes

depends critically on the nature of the relaxation processes. Saturation transfer spectroscopy depends on the spectral diffusion of saturation that occurs in time $T_1$ (spin-lattice relaxation time) because of modulation of anisotropic interactions by rotational diffusion. STESR method extend by several orders of magnitude the sensitivity of the spin label ESR to very slow motion of biological macromolecule, to the range from μs to ms. The basic idea of this technique is the "hole-burning", which is a well-known method in other spectroscopies, as well. It means the application of saturation power at one point of the anisotropic spectra, which is accord to an orientation of the molecule. The rate of reabsorption depends on the spectral diffusion of saturation, that varies across the spectrum according to the anisotropy of magnetic interactions. The saturation diffusion is effected by the rotational mobility of the macromolecules, therefore the resulted STESR spectrum is sensitive in shape to the rotational diffusion of the macromolecules. Hyde and Dalton in 1972 showed, that the spin-lattice relaxation of the nitroxyl radical moiety in the very slow tumbling domain is nearly independent of the motion. Similarly, the transverse relaxation processes (electron-nuclear and electron-electron dipolar interactions) affect the line shapes only slightly in the time range studied ($10^{-7}$s $\leq \tau_R \geq 10^{-3}$s). But for a shorter correlation times the nuclear relaxation may have a pronounced effect upon saturation transfer spectra. And to the mechanism responsible for loss of phase coherence and therefore contributing to $T_2$ (spin-spin relaxation time) must be added the effects arising from librational motions of the label *(Hyde & Dalton, 1976).*

In practice, there are four experimental methods to measure STESR spectra: progressive (or continuous wave) saturation; observation of the ESR dispersion signal, detected 90° out–of–phase with respect to the first harmonic of the field modulation; absorption, detected 90° out–of–phase with respect to the second harmonic of the field modulation; and the electron-electron double resonance (ELDOR). In fact, the second harmonic absorption out–of–phase is by far the most practical and widely used technique. In order to determine $\tau_R$ from STESR spectra the reference spectra must be determined at first by performing experiments on a model system (such as the spin labeled hemoglobin) in which correlation times can be determined from viscosity and temperature and structural data, or performing theoretical computer simulations (*Robinson & Dalton, 1980).*

Spectral parameters can be defined by the line-height ratio method, using the ratios of the low- (L"/L) center- (C'/C) and high-fields (H"/H) (see Fig.4) *(Thomas et al., 1976; Robinson & Dalton, 1980),* or the integrated ST-intensity *(Horváth & Marsh, 1983).* Accurate rotational correlation time can be determined by polynomial interpolation of the inverse function *(Horváth and Marsh, 1988; Marsh and Horváth, 1992).*

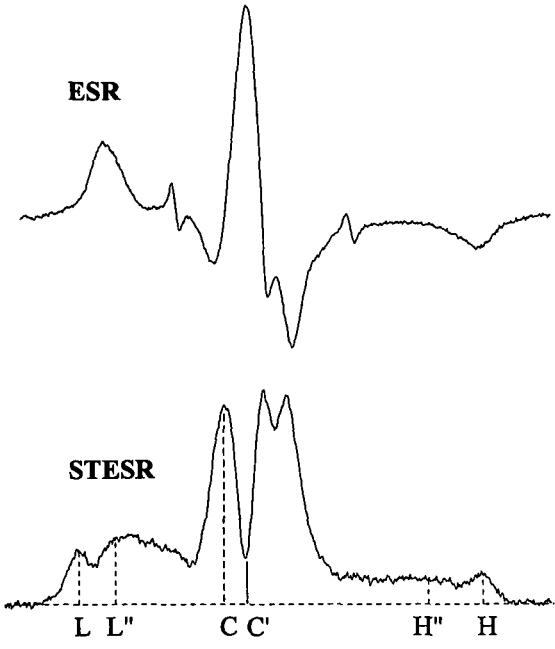


**Figure 4.** ESR and STESR spectra of spin-labeled $Ca^{2+}$-ATPase. H"/H is plotted, where H: is the height of peak near the high field turning point, H": is the height at a point intermediate between the two high field turning points; L"/L parameter is plotted, where L: the height of the peak near to the low-field turning point, L": is the height at a point intermediate between the two low-field turning points; and C'/C obtained from the central region of the spectrum *(Hyde & Dalton, 1976).*

# 4. Materials and Methods

*4.1 Chemicals and Preparation of SR Vesicles*

Analytical grade sucrose and glycerol were from Serva (Heidelberg, Germany) and Sigma (Munich, Germany), respectively. Spin labeled maleimides (5-MSL, 6-MSL) and spin labeled stearic acid (16-SASL) were from Sigma (Munich, Germany) and N-ethylmaleimide (NEM) was from Serva (Heidelberg, Germany), dissolved in dimethylsulfoxide (DMSO, Sigma-Aldrich, Munich, Germany). The 5-InVSL and $D_{13}$-$^{15}$N-5-InVSL spin labels kindly donated by K. Hideg were synthesized as described earlier *(Hankovszky et al., 1989)* and used in dimethylsulfoxide solution. Human hemoglobin, 2x crystallised, dialysed and lyophilised was purchased from Sigma (Munich, Germany). All other chemicals were of analytical grade purity and purchased from Sigma-Aldrich (Munich, Germany).

The $Ca^{2+}$-ATPase-containing sarcoplasmic reticulum vesicles were prepared from rabbit white skeletal muscles according to the method of Nakamura (*Nakamura et al., 1976*).

*4.2 Enzymatic Activity Assays and Negative Staining Electron Microscopy*

In the enzymatic activity and crystallization experiments the following solutions were used 0.1 M KCl, 10 mM MOPS (pH 7.4), 5 mM $MgCl_2$, 0.5 mM EGTA (Medium S) and 0 .1 M KCl, 10 mM imidazole (pH 7.4), 5 mM $MgCl_2$, 0.5 mM EGTA (Medium C) with 5 mM decavanadate, respectively. The $Ca^{2+}$,$Mg^{2+}$-activated ATPase activity was measured by colorimetric determination of liberated inorganic phosphate (*Nakamura et al., 1976; Eibl & Lands, 1969*). The rate of phosphate liberation from ATP was measured in Medium S supplemented with 0.45 mM $CaCl_2$ and 1 mM A23187 $Ca^{2+}$-ionophore at a protein concentration of 0.02 mg/ml at 25°C for 5 min. *(Dux & Martonosi, 1983a)*, with and without glycerol or sucrose. SR vesicle suspensions were divided into two aliquots for instant spin labeling with 5-MSL and parallel crystallization experiments, after a 24-hr-incubation period at 2°C in conjunction with electron microscopic measurements at this temperature. For negative staining the vesicle suspensions (1 mg of protein/ml) were placed on carbon-coated parlodion film and stained with freshly prepared 1% uranyl acetate (pH 4.3) at 2°C. Electron

micrographs were recorded with a JEOL 100-B microscope at 80 kV accelerating voltage *(Dux & Martonosi, 1983a).*

Essentially similar conditions were used for all enzymatic activity measurements, where we checked the effect of NEM prelabeling and spin labeling with MSL labels, 5-InVSL or $D_{13}$-$^{15}$N-5-InVSL

*4.3 Viscosity Measurements*

Viscosity of Medium S mixtures supplemented with sucrose or glycerol, and water-glycerol solutions used for the calibration of STESR parameters, were measured at several temperatures between 258K and 298K, using a thermostated rotating disc viscometer (Haake, Germany). For other temperatures the viscosities were calculated from the semilog plot of the viscosity of each glycerol solution *vs.* the reciprocal of the absolute temperature cubed *(Litovitz, 1952).*

*4.4 Spin Labeling*

$Ca^{2+}$-ATPase was prelabeled with NEM on the fast reacting interfacial *-SH* groups (group I) at a labeling level of 1:1 mol/mol for 5 min. *(Horváth et al., 1990).* Then, the intramembranous *-SH* groups (group II) were labeled with 5-MSL, in the presence of intercalated NEM, at a labeling level of < 1:1 mol/mol and of NEM for 40 min., and the unreacted NEM and spin labels were separated by centrifugation (Beckman 50Ti at 40,000 rpm) for 30 min. Spin labeled stearic acid (16-SASL) was intercalated into SR membrane prior to the addition of polyols and incubated at ambient temperature (25°C) for 15 minutes before removing the non-intercalated spin probes by low-speed centrifugation.

Hemoglobin (1mM) was labelled with 5-InVSL (2mM) in physiological NaCl buffer, for 40 min at room-temperature. Then either the excess spin labels were removed using gel filtration (Sephadex G-25) or $NiCl_2$ in 20 mM concentration was used as a paramagnetic quencher.

*4.5 ESR studies*

ESR spectra were recorded on a Bruker ECS 106 Series 9 GHz spectrometer equipped with a temperature regulation system based on pressured air gas flow. Spin labeled $Ca^{2+}$-ATPase rich vesicles were packed in 1 mm I.D. capillaries by low-speed centrifugation. Temperature was measured by a fine-wire thermocouple located at the bottom of the microwave cavity within the Dewar insert. Conventional ($V_1$-display) and saturation transfer ($V_2$'-display) ESR spectra were recorded using 100 kHz and 50 kHz modulations using the recommended protocol for STESR measurements *(Hemminga et al., 1984).* In the most cases the signal-to-noise ratio of the STESR spectra was improved by smoothing over a 5-point-window at low field, a 3-point-window in the center, and a 7-point-window at high field in the case of line height ratio measurements. (It should be noted that the anisotropy in the three regions are 2.18, 1.01, and 3.70 mTesla, respectively.) Spectral amplitudes of the diagnostic points (L, L", H, and H") of STESR spectra were evaluated as described earlier (*Robinson & Dalton, 1980)*, and calibrations of STESR line height ratios (L"/L and H"/H) and normalized STESR intensities of MSL-, 5-InVSL- or $D_{13}$-$^{15}$N-5-InVSL-labeled hemoglobin were taken from the literature *(Horváth & Marsh, 1988; Marsh & Horváth, 1992; Robinson & Dalton, 1980)* and from own calibration (5-InVSL).

## 5. Results and Discussion

*5.1 Influence of aqueous viscosity on the enzymatic activity and crystallization of $Ca^{2+}$-ATPase.*

The enzymatic activity of $Ca^{2+}$-ATPase was sharply reduced on increasing the viscosity of the aqueous phase. However, as shown in Fig. 5., after the addition of sucrose or glycerol to the aqueous phase the relative activity was reduced to different extent. As the viscosity was increased from 1.1 to 13.2 mPa·s ($1\times10^{-3}$ Pa·s=$1\times10^{-2}$ Poise) by adding glycerol the relative activity of the enzyme was reduced to 0.12, whereas on increasing the viscosity from 1.1 to 12.0 mPa.s by the addition of sucrose the relative activity was reduced to lesser extent, to 0.64. As to the analytical form of the viscosity induced relative activity reduction, in the case of sucrose the decline in relative enzymatic activity varied according to the inverse power law, ~ $1/\eta^b$ , with b=0.21, typical for non-interacting solvents *(Kramers, 1940)*. Glycerol, on the other hand, led to an exponential activity decay, ~ $e^{-b\eta}$ with b=0.17 indicating interaction between the solvent molecules and the extramembranous part of the polypeptide; a more complete discussion for proteins of the plasma membrane is given in references *(Bérczi & Moller, 1993)*. For the sake of comparison the complementary forms of the viscosity dependence, namely exponential curve for sucrose and inverse power law for glycerol, are also shown in Fig. 5. Less acceptable fits were obtained with typical root-mean-square (R.M.S.) values of 97.2 % versus 94.5% in the case of sucrose for fitting according to power law and exponential decay, and 89.2% versus 99.5% in the case of glycerol for fitting according to power law and exponential decay, respectively.

Crystalline arrays of $Ca^{2+}$-ATPase from native SR induced by vanadate were formed in the presence of glycerol, and essentially very similar arrays were obtained after the addition of glycerol to preformed 2D-crystals of the enzyme by negatively stained SR in agreement with previous results (EM pictures not shown, *Dux, 1993*). As demonstrated by EM neither the incorporation of spin labels *(Lewis & Thomas, 1986)* nor glycerol had any effect on 2D-crystal formation, at least using negative staining EM at low resolution. In previous reports of multilamellar crystals of detergent solubilized $Ca^{2+}$-ATPase it was suggested that glycerol has an inhibitory effect on in-plane nucleation, but crystal fusion after nucleation was facilitated

*(Varga et al., 1991; Sji et al., 1995; Cheong et al., 1996).* As known from crystallization experiments the presence of glycerol does not influence the formation of peptide-bridges which are essential in building-up of protein crystals *(Taylor et al., 1986; Napolitano, 1983).* Implicit to these crystallization experiments is that the molecular dimensions are not greatly perturbed by the presence of glycerol molecules; the effect of sucrose on crystallization is discussed later.

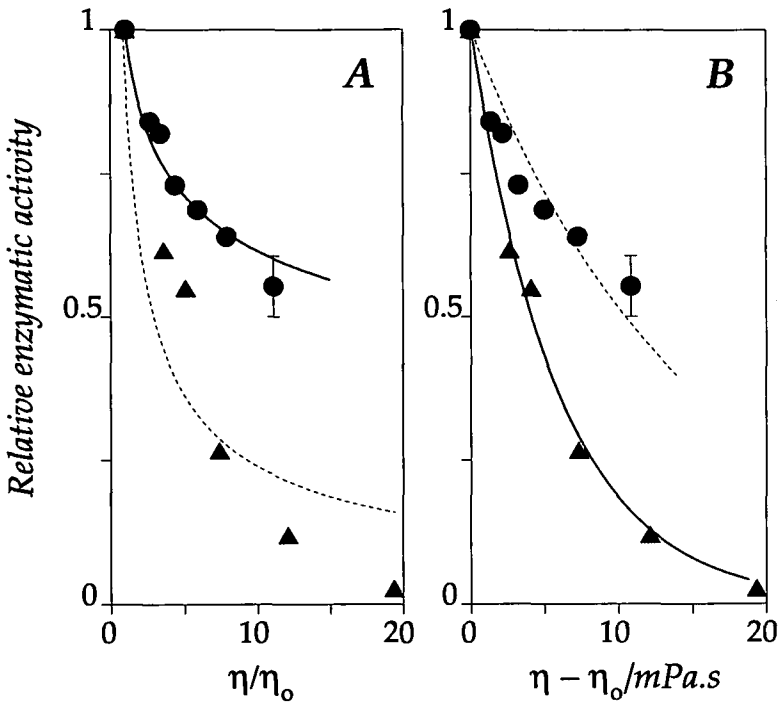


**Figure 5.** The relative enzymatic activity of $Ca^{2+}$-ATPase as a function of the viscosity of the aqueous phase and best fitting curves assuming reciprocal power law ~ $1/\eta^b$ (A) and exponential decay law ~ $e^{-b\eta}$ (B) for calculation. Best fitting coefficient values were b=0.21 in the case of sucrose (●–●–●) and b=0.17 in the case of glycerol (▲–▲–▲); the root-mean-square error (R. M. S.) of fitting of inverse power law for sucrose (solid line in Panel A) was 97.2%, while for glycerol the R. M. S. error was 99.5% (solid line in Panel B). Best fitting complementary curves in these cases (dashed lines) gave significantly worse fits. For sucrose assuming the exponential decay law with b=0.066 an R.M.S. error of 94.5%, while for glycerol assuming inverse power law with b=0.62 an R.M.S. error of 89.2% was obtained.

### *5.2 Effect of the Increased Viscosity on the Rotational Mobility*

#### *5.2.1 Conventional ESR spectra.*

On labeling $Ca^{2+}$-ATPase with spin labeled maleimide (5-MSL), after brief prelabeling of the fast reacting interfacial *-SH* groups (group I) with NEM, a strongly immobilized line shape was obtained indicating no significant segmental motion of the spin label when covalently bound (group II, *Hidalgo & Thomas, 1977*). It should be noted that spin labeling experiments were done at 20°C in a short time (<1 hour). The ubiquitous weakly immobilized component, which unlike the immobile component could be quenched by $Ni^{2+}$ ions and, thus, assigned to covalently attached labels at the interface of the lipid bilayer or intercalated, but unbound spin labels in the intramembranous phase, was reduced to < 5% in a single washing

step. The hyperfine splitting, $2A_{max}$, and the line widths at half-height, $H_{low}$ and $H_{high}$, of the outer extrema (spectra not shown) were 68.0 Gauss, 3.0 Gauss, and 3.8 Gauss, respectively. It should be noted that the line width data depended on the labeling level and, thus, the $MSL_{bound}$/ $Ca^{2+}$-ATPase molar ratio was kept constant at 0.75 mol/mol. The obtained spectral parameters agreed with previous results on label/protein stoichiometry experiments *(Horváth et al., 1990)*. Since all spectra were close to the rigid limit line shape more quantitative experiments required STESR methods which have a time scale of $10^{-6}$-$10^{-4}$s.

The intramembranous viscosity of the center of the lipid bilayer was followed by spin labeled stearic acid (16-SASL) intercalated prior to the addition of polyols to the aqueous phase. The rotational correlation time of spin labeled stearic acid was $1.41\pm0.02\times10^{-9}$s as measured by the line width method *(Schreier et al.,1978)*. After the addition of sucrose or glycerol by increasing the aqueous viscosity of the extramembranous phase from 1.1 mPa.s to 12.0 or 20.5 mPa·s the correlation time remained unchanged: $1.40\times10^{-9}$s and $1.38\times10^{-9}$s, respectively in agreement with previous work *(Squier & Thomas, 1988)*.

*5.2.2 Saturation transfer ESR spectra*

A series of second-harmonic, 90° out-of-phase ($V_2'$) STESR spectra of covalently labeled 5-MSL + $Ca^{2+}$-ATPase in Medium S supplemented with sucrose or glycerol of increasing viscosity is shown in Fig. 6. The signal-to-noise ratio of these spectra were improved by smoothing over 5/3/7-point-window in the low-field, central, and high-field region and the signal-to-noise ratios were (at least) 8:1, 16:1, 3:1 and 18:1, 28:1, 8:1 in the untreated and smoothed spectra, respectively. On increasing the viscosity of the extramembranous phase progressive changes were observed in the line shapes of STESR spectra and, in particular, in the line heights in the diagnostic regions at low and high fields. All these spectra were obtained at the same labeling level ($MSL_{bound}$ / $Ca^{2+}$-ATPase = 0.75 mol/mol) in order to control the effect of spin-spin interaction which was shown to influence selectively the normalized STESR intensity *(Horváth et al., 1990)*..

As the viscosity of the aqueous phase was increased from 1.1 to 12.0 mPa·s and 20.5 mPa·s by adding 50 w/v% sucrose and 74 w/v% glycerol at 20°C, respectively, the diagnostic line height ratios, which are sensitive to the rotational correlation time *(Squier & Thomas, 1986),* were increased from L"/L=0.29 to 0.94 and H"/H=0.30 to 0.86 as expected for slowing molecular rotation.

The low-field (L"/L) and high-field (H"/H) line height ratios were determined and compared to spin labeled hemoglobin calibrations *(Horváth & Marsh, 1988; Marsh & Horváth, 1992).* The difference between the correlation time values from low-field and high-field line height ratios were < 10-25% provided the signal-to-noise ratios allowed such comparisons. As a rule, the low-field line height ratio (L"/L), after smoothing over a 3-point-window, was more affected by the overlapping mobile spectral component (Fig. 6). It should be noted that the experimental error in determining the STESR line height from the high-field region (H"/H) was filtered by smoothing over a 7-point-window. The extramembranous height was estimated from average values obtained in low-field and high-field STESR measurements. The correlation time had an uncertainty of $2.5 \times 10^{-6}$ s yielding a propagated error in the height data of $5 \times 10^{-10}$ m. Qualitatively similar spectral changes were reported by Lewis and Thomas *(Lewis & Thomas, 1986)* and Napier et al. *(Napier et al., 1987)* for STESR spectra of covalently labeled $Ca^{2+}$-ATPase in two-dimensional $E_2$ crystalline form.

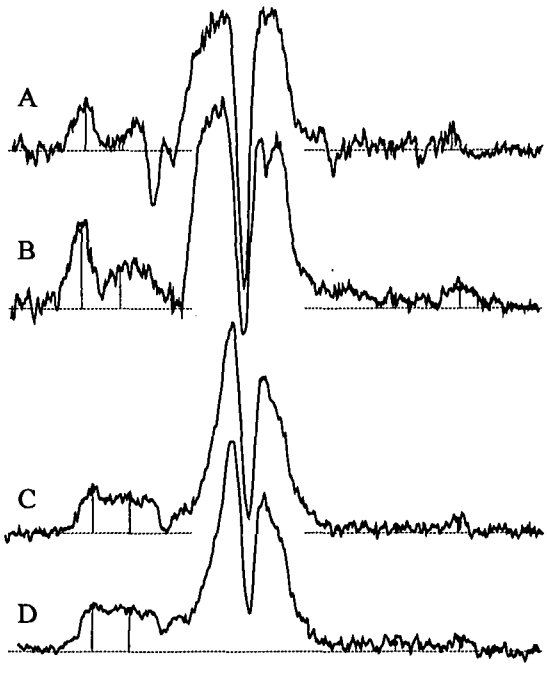


**Figure 6.** Second harmonic, 90° out-of-phase absorption ($V_2'$) STESR spectra of covalently labeled sarcoplasmic reticulum vesicles at a labeling level of 5-MSL:$Ca^{2+}$-ATPase=0.75 mol/mol and adding various amounts of sucrose or glycerol to Medium S and using the noise filter of 5-point-window method. (A) Spin labeled SR vesicles in Medium S; (B) 50 w/v% sucrose and Medium S; (C) 52 w/v% glycerol and Medium S; (D) 64 w/v% glycerol and Medium S. Total scan width was 10 mTesla and the temperature was 293 K.

*5.2.3 Hydrodynamic model*

The leading term in the rotational correlation time $\tau_R$ is the contribution to the correlation time due to the intramembranous part $\tau_{R,m}$ which varies with the intramembranous viscosity in the range of $\eta_m$=200-500 mPa·s *(Cherry & Godfrey, 1981)* and the contribution of the extramembranous part in the aqueous phase (1.1 mPa·s) is usually neglected to first approximation, i. e. $\tau_R \approx \tau_{R,m}$. Eq. (5) (in page...) is based on two assumptions: namely, (1) the torque due to the intramembranous and extramembranous parts of the enzyme consists of additive, almost collinear, vectors *(Feynman et al., 1963)* and, hence, the increase in rotational correlation time is linearly proportional to the viscosity of the aqueous phase, and (2) the extramembranous and intramembranous segments are rigidly connected. This assumption is certainly applicable in the case of $Ca^{2+}$-ATPase according to recent three-dimensional modeling *(Taylor et al., 1986a; Toyoshima et al., 1993)*. A simplifying assumption, in agreement with three-dimensional reconstruction of the enzyme in $E_1$ and $E_2$ forms, is that the ellipticity factor is uniform across the various parts in different viscous phases. According to morphological data the ellipticity factor is 0.87 and will only change by the formation of two-dimensional aggregation *(Horváth et al., 1990)*. The 'pear-shaped' molecule has no large extensions

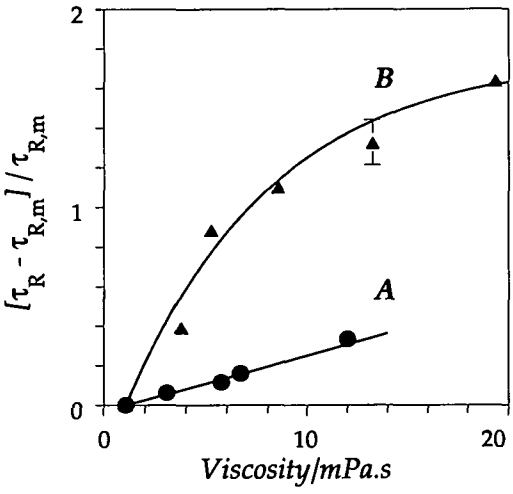


**Figure 7.** The normalized effective correlation time increase of covalently labeled $Ca^{2+}$-ATPase as a function of aqueous phase viscosity after the addition of sucrose (A, ●–●–●) or glycerol (B,▲–▲–▲). The correlation times were determined from the combined application of the low-field (L"/L) and high-field (H"/H) line height ratios of STESR spectra. The measured points for sucrose are shown together with a best fitting straight line (solid line) following Eq. (7) in the interval of $\eta$= 0-12 mPa·s and for glycerol with a logarithmic curve in the interval of $\eta$= 0-20 mPa·s.

either in the intramembranous or extramembranous parts suggesting an evenly round mobile contour *(Taylor et al., 1986b)*. Strictly speaking the effective correlation time is related to the diffusion tensor and the orientation of NO-group, as discussed earlier *(Robinson & Dalton, 1980)*. By paramagnetic quenching of transition ions, like nickel soluble in the aqueous phase, it has been shown that the spin label has covalently been attached to *-SH* groups in the intramembranous part of the enzyme molecule prior to the addition of polyols and it is assumed that the orientation of spin label is not modified by the aqueous viscosity. In this

case the ratio of the correlation times prior to and after the addition of viscous polyols is not dependent on the orientation of the label.

For quantitative evaluation an experimental parameter was introduced normalizing the measured correlation time increase ($\tau_R$-$\tau_{R,m}$) with that due to the intramembranous contribution $\tau_{R,m}$. (Eq. 7). The viscosity dependence is determined, according to Eq. (7), by the viscosity of the intramembranous phase and the measured values for various membranes specify a range of 200-500 mPa·s *(Cherry & Godfrey, 1981)*. At the lower and upper limits, assuming equal heights for the intramembranous and extramembranous segments $h_m = h$, for the slope values of the $(\tau_R - \tau_{R,m})/\tau_{R,m}$ *vs.* $\eta$ curves 0.015 $(mPa \cdot s)^{-1}$ and 0.006 $(mPa \cdot s)^{-1}$ are expected, respectively. The measured slope of the $(\tau_R-\tau_{R,m})/\tau_{R,m}$ *vs.* $\eta$ curve was 0.0235(5) $(mPa \cdot s)^{-1}$ on increasing the viscosity of the aqueous phase by the addition of sucrose (Fig. 7). Thus, the ratio of the two segments is related to the membrane thickness as $h/h_m \sim 1.6$ and 3.9 at the lower and upper limits of intramembranous viscosity ranges, respectively. Assuming a membrane thickness of $\eta_m$ = 4.5 nm, this measurement gives for the height of the extramembranous segment $h$ = 6.8 nm and 17 nm at the lower and upper limits of the viscosity range, respectively. Accordingly 82% - 92% of the volume of the volume of $Ca^{2+}$-ATPase protein is external to the sarcoplasmic reticulum. The value at the lower limit of intramembranous viscosity range is in good agreement with previous data obtained from low-resolution diffraction and three-dimensional molecular reconstruction estimates *(Andersen, 1989)*. It should be noted that the calculated height of the extramembranous segment depends on the value of intramembranous viscosity and, thus, fluidity modulation due to temperature changes or alteration in the concentration of membrane soluble drugs could modify the size of protruding segments.

There are two independent lines of indications that glycerol and sucrose exert qualitatively different alterations on interacting with $Ca^{2+}$-ATPase. In the case of these polyols, although both inhibited enzymatic activity, qualitatively different viscosity dependencies were observed. Large concentrations (> 0.5 M) of sucrose have prevented the formation of decavanadate induced $E_2$ crystals, whereas 40 w/v% glycerol even improved the self association of the solubilized enzyme *(Varga et al, 1991)*. The simple linear dependence on viscosity predicted by Eq. (7), which has given a consistent explanation of correlation time

and enzymatic activity data for sucrose, does not give an acceptable fit for glycerol (cf. Figs. 5 and 7). In addition, glycerol is a generally used polyol to facilitate the polymerization of crystal patterns of solubilized $Ca^{2+}$-ATPase *(Varga et al., 1981; Varga et al., 1986)*, whereas sucrose was a polyol supplement which at low concentrations (up to 0.4 M) had no effect on two-dimensional (2D) crystal formation in native SR, while at high concentrations (0.5-1 M) abolished the process *(Dux & Martonosi, 1983)*.

The correlation time data evaluated from STESR line height parameters display similar correlation time increases on adding glycerol for varying the viscosity, but the observed changes were both quantitatively and qualitatively rather different from that measured after the addition of sucrose. The effective correlation times of covalently labeled $Ca^{2+}$-ATPase in glycerol suspensions are much greater than those in sucrose suspension of the same viscosity suggesting the formation of larger protein aggregates. Alternatively, the height of the extramembranous fraction ought to be increased by a factor of $\sim 5$ on expense of the intramembranous fraction; this is in contradiction with the balance of hydrophobic forces. It should be noted that the addition of glycerol, which leads to the formation of such aggregates, could serve as an effective enzyme inhibitor in agreement with the steeply declining activity data. As another mechanism, namely the effect of dehydration due to solute/protein interaction is discussed by Esmann et al. *(Esmann et al., 1994)*.

*5.3 Notes on the Chemistry of the 5-InVSL Spin Label*

*5.3.1 Comparative Studies with $^{14}N$, $^{15}N$ 5-InVSL Spin Labels*

The effect of aqueous viscosity on conventional and STESR spectra of $^{14}$N-5-InVSL or $D_{13}$-$^{15}$N-5-InVSL attached to $Ca^{2+}$-ATPase are shown in Fig. 8. The effective rotational correlation time, $\tau_R^{eff}$, measured by saturation transfer ESR depends on the orientation of the spin label (Eq. 4). Chemical structures ( Fig. 2) of maleimide type (5-MSL, 6-MSL) and so-called indane dione type spin labels (5-InVSL, $D_{13}$-$^{15}$N-5-InVSL) in agreement with STESR spectra (Fig. 8) suggest that latter spin labels can more rigidly attach to the biological macromolecules. In the case of $Ca^{2+}$-ATPase the line-height ratios of L"/L=1.18±0.02 and H"/H=0.78±0.02 were obtained for $^{14}$N-5-InVSL at 278K without glycerol, giving effective rotational correlation times of $\tau_R^{eff}=8.8\times10^{-5}$ s and $6.5\times10^{-5}$ s, respectively. Essentially similar data were obtained for $Ca^{2+}$-ATPase labeled with $D_{13}$-$^{15}$N-5-InVSL, the line-height ratios were L"/L=1.14±0.02 and H"/H=0.73±0.01 giving effective rotational correlation times of $6.5\times10^{-5}$ s and $5.5\times10^{-5}$ s, respectively. In both cases the used calibration curves based on computer simulations. *(Robinson and Dalton, 1980).* According to the literature data, for the monomer of $Ca^{2+}$-ATPase enzyme (F≈1) a long-axis rotational correlation time of $\tau_{R\|}=2.5\text{-}5\times10^{-5}$s is expected, and for the dimer (F≈0.8) the predicted rotational correlation time is $6\times10^{-5}$-$1.2\times10^{-4}$s. The measured effective rotational correlation times for $^{14}$N-5-InVSL are in agreement with these predictions provided the nitroxyl axes are oriented within an angular range of Θ=25°-45° to the rotational axes *(Horváth et al., 1990).* Spin label ESR measurements of MSL attached to $(Na^+,K^+)$-ATPase reported a value of $2.5\times10^{-5}$s for the long-axis rotational correlation time and the above estimates yielded $1.6\text{-}3.4\times10^{-5}$ s with the

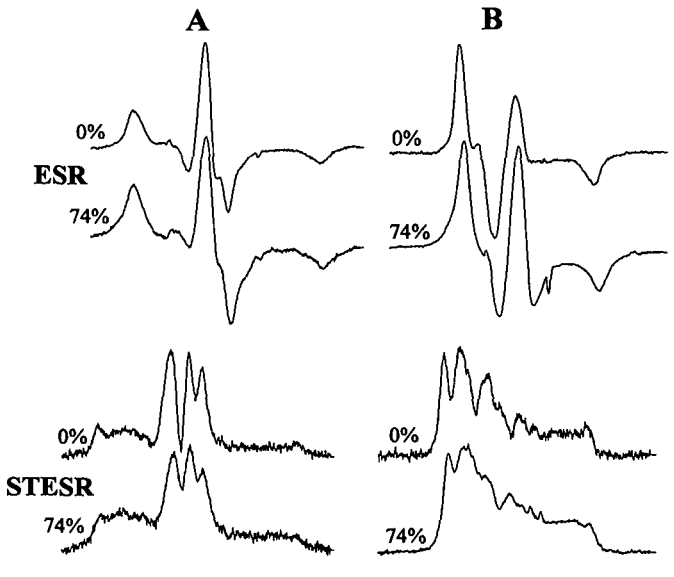


**Figure 8.** Conventional and saturation transfer ESR spectra of $^{14}$N- (column **A**) and $^{15}$N- based (column **B**) spin labels attached to intramembranous -SH groups of $Ca^{2+}$-ATPase in the presence of 0 w/w% or 74 w/w% glycerol, at 277 K. Total scan width is 10 mT.

assumption of $\theta=90^{o}$ orientation and an oligomer form of dimer *(Esmann et al., 1987).* The effect of segmental motion of both groups of spin labels mentioned above were checked in the case of $Ca^{2+}$-ATPase by Horváth *et al.* They found that MSL spin label displayed considerable segmental mobility relative to the whole protein when covalently bound to the $Ca^{2+}$-ATPase. In contrast to MSL, the 5-InVSL spin label were very well suited to STESR studies of the overall rotational diffusion of the proteins, because of favorable reactivity and lack of independent segmental motion *(Horváth et al., 1990)*. However, the hopefully applicability of these indane dione type spin labels, arising from substantially different orientation and more rigid binding, are limited because of the difficulties (*vide infra*) of empirical calibration of STESR spectral parameters.

Comparing the $Ca^{2+}$-ATPase, as an integral membrane protein, and the water soluble hemoglobin used for the calibration of STESR spectral parameters of 5-InVSL, several notable differences were observed in the labeling processes. The observed behaviors can be used as an advantage, as well, to characterize the accessibility of the labeling sites of the proteins.

### *5.3.2 Accessibility of Protein Sulfhydril Groups to Nitroxyl Spin Labels*

The labeling processes are based on a Michael-type addition (Scheme 1). In the case of the former maleimide-type spin labels (5-MSL and 6-MSL), as a rule, the retro-reaction, i.e. label release, can generally be neglected. A member of the advanced generation of spin labels, the 5-InVSL, which is more rigidly attached to the peptide molecules, due to its bulky planar side group and anchoring capability of oxo groups to protein via hydrogen bonding. These novel bonding properties allow site-specific tagging of other classes of sulfhydryl groups

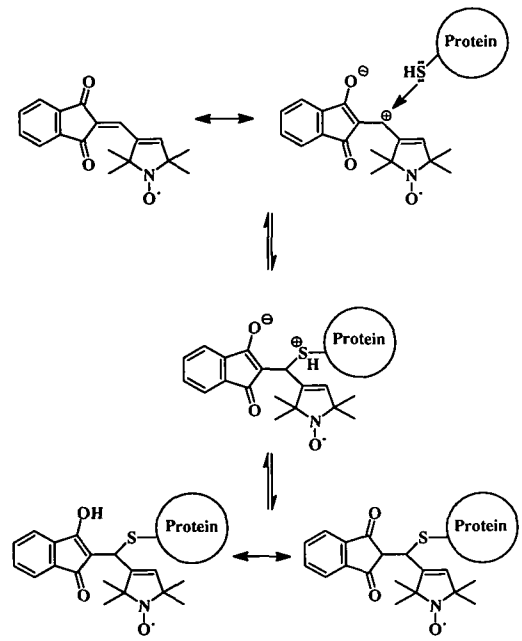


**Scheme 1.** One of the possible mechanisms for binding the spin label to the sulfhydryl groups of the protein by Michael-addition.

*(Esmann et al., 1993).* An universal, hitherto unconsidered phenomenon has been observed by ESR spectroscopy on comparing the labeling of an integral membrane protein, the $Ca^{2+}$-ATPase of sarcoplasmic reticulum (M.W. 113 kD), with a water soluble protein, the hemoglobin (M.W. 63kD): the retro-Michael reaction was rather different in these two cases. More specifically, there was no label release during $Ca^{2+}$-ATPase labeling even after 40 minutes labeling at room temperature and a subsequent overnight incubation at 4°C, whereas a fast retro-Michael reaction was observed in the case of hemoglobin even during the labeling time at ambient temperature.

The ESR spectra of labeled $Ca^{2+}$-ATPase and hemoglobin were qualitatively similar consisting of a rigid limit component of full spectral anisotropy and a motionally averaged isotropic component. As in similar systems, the rigid limit line shape can be assigned to nitroxyls covalently attached to sulfhydryl group(s) of the polypeptides, whereas the presence of the isotropic spectral component indicates free nitroxyl molecules prior to covalent binding or after label release due to the retro-Michael reaction. A typical spectrum series is shown in Fig. 9. After the covalent binding, the unreacted spin labels, which are marked by the isotropic three spectral lines, were removed by column chromatography (Fig. 9A). However, the retro-Michael reaction was observed on covalently labeling the β93 -SH group of hemoglobin by 5-InVSL, the initially small mobile component reappeared rapidly in few minutes (Figs. 9B-D).

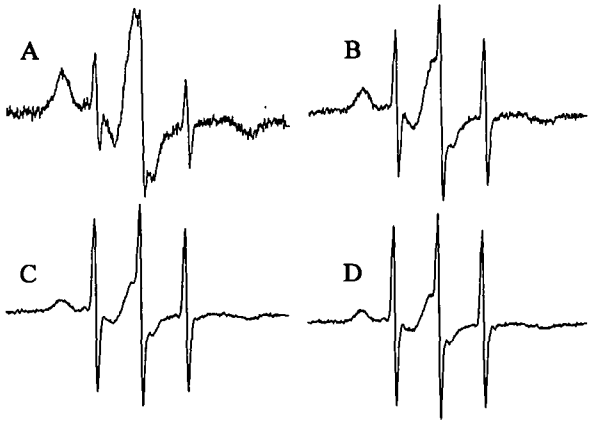


**Figure 9.** Covalent binding of 5-InvSL in the nonpolar phase of hemoglobin by the Michael reaction and the release of already bound labels by the retro-Michael reaction. After removal of unreacted spin labels using column chromatography (A). Label release after 60 s (B), 91 s (C), 139 s (D). Scan range 10mT.

Qualitatively similar, but quantitatively very different spectrum series was obtained in the case of $Ca^{2+}$-ATPase (Figs 10A-B). In addition, similar spectra were obtained for structurally related spin label compounds where the five-member N-oxyl radical ring is attached via a propenone chain to relatively bulk groups, such as phenyl, pyridinium, hydroxyphenyl, azidophenyl, and benzoyl (spectra not shown).

For quantitative comparison, the two-component spectra were evaluated by digital subtraction and double-integration of the baseline-corrected ESR spectra, these fractional integrated intensities are proportional to the concentrations of the spin label. Most of the spin labels remained attached to the $Ca^{2+}$-ATPase, only in 0.5% released after 25 hours. However, in the case of hemoglobin 96.5% of the spin labels were immobilized after the gel-filtration and this value decreased to 88%, 79%, 75%, and 70.5% after 60 s, 91 s, 139 s and 3 days, respectively. As a result, in 5-InVSL calibration with hemoglobin, the correct evaluation of the spectra is very difficult because of their mobile components (Figs. 10C-D). Small pH-changes (pH=6, pH=8) or adding structurally identical, but non-ESR active compounds to the sample after the filtration were ineffective to obtain better ESR spectra. Thus, as an alternative procedure, namely, paramagnetic quenching was applied which selectively removes the unreacted spin labels from the aqueous phase and left the covalently bound labels unchanged since nickel ions are impermeable to the nonpolar interior of hemoglobin. In such cases saturation transfer ESR could be performed by quenching the mobile peaks (Figs. 10E-F). The labeling sulfhydryl sites are located in different parts of the polypeptides in the above two cases. In hemoglobin the sole sulfhydryl group (β93) is in a compact nonpolar structure and so the

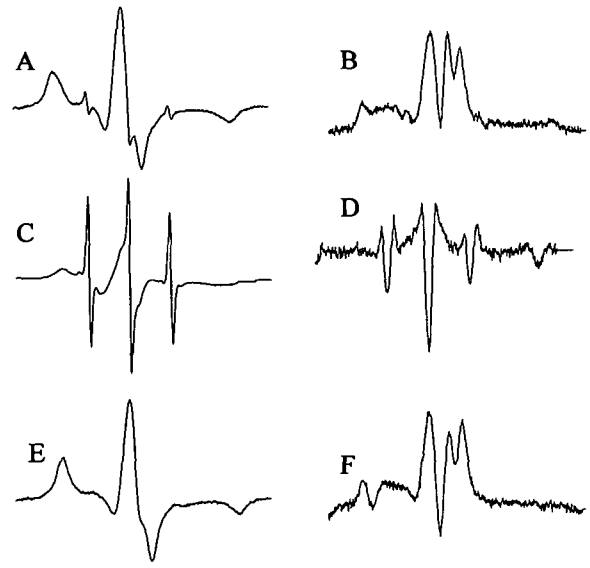


**Figure 10.** Conventional and saturation transfer ESR spectra of 5-InVSL covalently attached to sulfhydryl groups of $Ca^{2+}$-ATPase, and hemoglobin prior to and after paramagnetic quenching of unreacted nitroxyls by 20 mM $Ni^{2+}$. Conventional ESR spectra of the spin labeled $Ca^{2+}$-ATPase (A) and hemoglobin (C). Saturation transfer ESR spectra of spin labeled $Ca^{2+}$-ATPase (B) and hemoglobin (D). Parallel conventional (E) and saturation transfer ESR spectra of spin labeled hemoglobin in the presence of nickel ions.

bulk 5-InVSL molecule has limited access to the labeling site and, hence, label binding is less complete and label release will be dominant. In $Ca^{2+}$-ATPase, on the other hand, the labeling sites (Cys610, 612, etc.) are in a less compact intramembranous region and so the geometrical constraint for the same spin label is less critical offering thereby more complete access and binding.

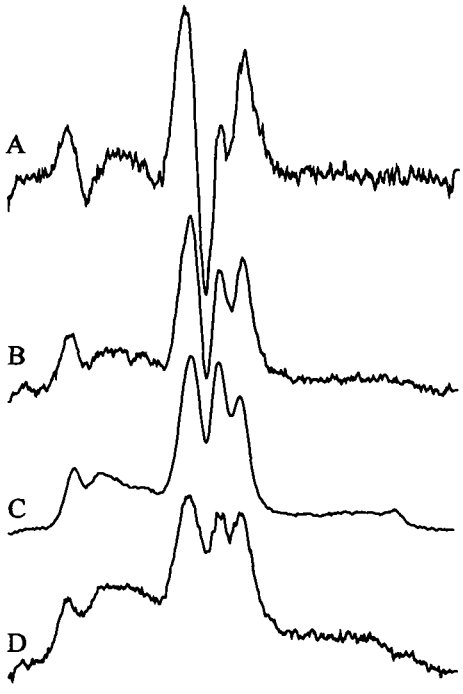


**Figure 11.** Reference STESR spectra of 5-InVSL labeled hemoglobin: at 298K in water (A); at 268K in 60 w/w% glycerol (B); at 288K in 92 w/w% glycerol (C); at 243 K in 92 w/w% glycerol solutions. Scan range 10 mT.

*3.5.3.3 Calibration of the STESR Parameters of 5-INVSL-labeled Hemoglobin*

As a consequence, paramagnetic quenching was used to mask the spectral contributions from unbound spin labels to the reference STESR spectra of spin-labeled hemoglobin (Fig. 11) instead of removal by spectral substractions *(Roopnarine, 1993).* Thus, calibration of STESR spectral parameters could be carried out as it is shown in Fig. 12. The model system samples corresponding to known rotational correlational times, were prepared with solution of liophilized 5-InVSL-labeled in different glycerol/water mixtures. The rotational correlation times were calculated from the Stokes-Einstein-Debye equation:

$$\tau_R = 4\pi r^3 \eta / kT \qquad (8),$$

where $\eta$, is the solution viscosity (Fig. 12); *T,* is the absolute temperature; *k,* is Boltzmann's constant and *r*, the radius of hemoglobin assumed to be $r$=2.9 nm. Accurate correlation time can

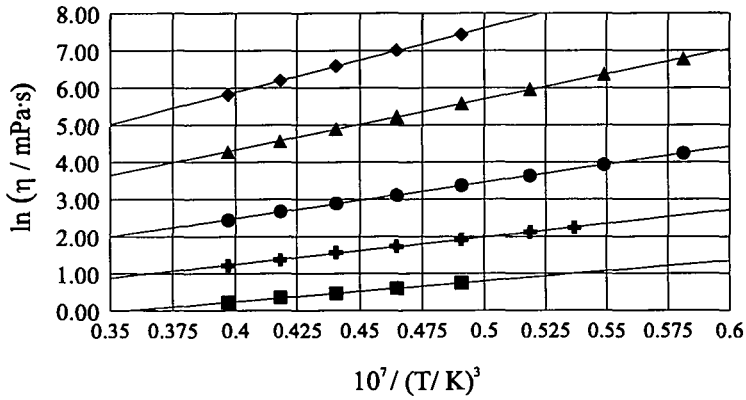


**Figure 12.** Viscosity (η) of glycerol solutions as a function temperature (T). The labels mean 5 w/w % (■), 36 w/w % (+), 60 w/w % (●), 80 w/w % (▲), and 90 w/w % (♦) glycerol concentrations.

be determined by polinomial interpolation of the inverse semilogaritmic function *(Horváth & Marsh, 1988; Marsh & Horváth, 1992).* Best fitting curves and coeffitient values are shown in Fig. 13. The rotational correlation time can be calculated as

$$\lg \tau_R(x) = \sum_{i=0}^{3} a_i x^i \qquad (9).$$

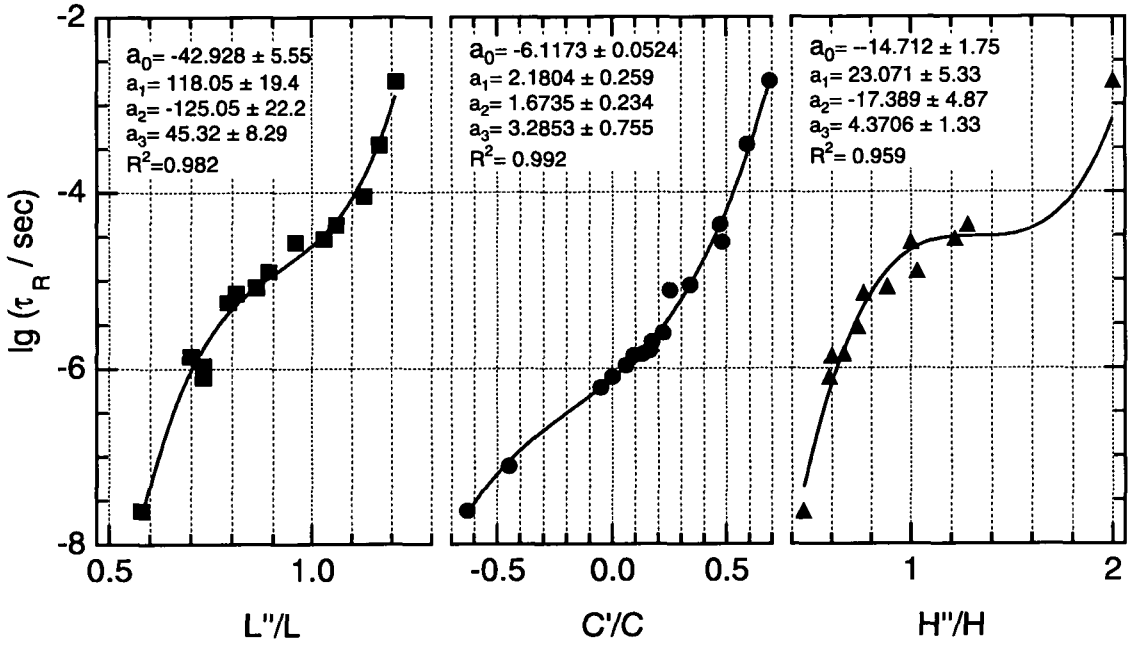


**Figure 13.** Least square fitting curves and polinomial coeffitients ($a_0+a_1x+a_2x^2+a_3x^3$) for calibrations of 5-InVSL STESR parameters. Lineheight-ratios in the low- (L"/L), center- (C'/C) and high-field diagnostic regions.

## 6. Conclusions

1. The modulating role of extramembranous segments to rotational mobility in viscous media is considered and saturation transfer ESR spectroscopy is used for mapping the extramembranous dimensions of transmembrane proteins. Finally the effect of viscosity of the aqueous phase and protein-protein interaction is discussed in light of two selected examples. The effective rotational correlation time of the protein increased linearly with the viscosity of the sucrose containing medium giving an extramembranous height of 6.8 nm. Glycerol, as indicated by the greater changes in rotational mobility led to the formation of larger aggregates. In the case of sucrose the ATP hydrolyzing activity of the enzyme has a reciprocal power dependence of viscosity, in agreement with previous results for non-interacting solvents, while glycerol caused a hitherto not observed exponential decay (*cf.* Török *et al.* BBA 1997).

2. Comparing the labeling processes of an integral membrane protein, the $Ca^{2+}$-ATPase and the water soluble hemoglobin, significant differences were observed. In conclusion it has been found that the structure of the covelent label and, in conjunction, the molecular geometry of the sulfhydryl site will determine the rates of Michael and retro-Michael reactions and, hence, the accessibility of the labeling sites. Paramagnetic quenching is proposed for the calibration of spectral parameters used in saturation transfer ESR of spin labeled hemoglobin with 5-InVSL, to mask the signals of nitroxyls released via the retro-Michael reaction (*cf.* Török *et al.* JMR 1997).

## 7. Acknowledgments

I gratefully thank for a 3-years doctoral fellowship to Ministry of Education. This work was additionally supported by grants from Hungarian National Science Foundation ( OTKA T6277/1993, OTKA T13257/1994), Soros Foundation and Hungarian Biochemical Society.

I greatly acknowledge to Professor László Dux, Dr. Pál Ormos and Professor George A. Olah for providing opportunity to work at their institutes. I really appreciate to the members of the Department of Biochemistry (SZOTE, Szeged), Institute of Biophysics (BRC, Szeged) and Loker Hydrocarbon Research Institute (USC, Los Angeles) for their help and friendship.

I greatly indebted to my tutors, Professor László Dux and Dr. László Horváth for their scientific guidance, encouragement and support they gave me during these years.

Thanks are due to Dr. Györgyi Jakab, Gerda Szakonyi, Zita Felhõ and Csilla Erndt for enzymatic activity measurements, electron microscopic experiments and their help in membrane preparations. Special thanks to Professor Kálmán Hideg for spin label molecules, Dr. Alajos Bérczi and Dr. Tibor Páli for their useful notes to the interpretation of the results. The usage of rotating disc viscometer is gratefully acknowledged to Professor Imre Dékány.

I am especially thankful to Dr. Béla Török, my husband and co-author in several publications, to my daughter, Fanni and to my parents for their invaluable help and patient.

## 8. References

Abney, J. R. and Owicki, J. C. (1985) Theories of protein-lipid and protein-protein interactions in membranes. *In* Progress in Protein-Lipid Interactions, Watts, A. and de Pont, J. J. H. H. M., editors.Vol. 1, Elsevier, Amsterdam, 1-60.

Andersen, J. P. (1989) Monomer-oligomer equilibrium of sarcoplasmic reticulum Ca-ATPase and the role of subunit interaction in the $Ca^{2+}$ pump mechanism. *Biochim. Biophys. Acta* **988**, 47-76.

Bérczi, A. and Moller, I. M. (1993) Control of the activity of plant plasma membrane MgATPase by the viscosity of the aqueous phase. *Physiol. Plantarum* **89**, 409-415.

Berliner, L. J. (1978) Spin labeling in enzimology: spin-labeled enzymes and proteins *Methods in Enzimology* **49**, 419-479.

Berliner, L. J., ed. (1976, 1979, 1989) Spin Labeling Theory and Applications. Vol. I-III., Academic Press, New York.

Bigelow, D. J.and Inesi, G. (1992) Contributions of chemical derivatization spectroscopic studies to the characterization of the $Ca^{2+}$ transport ATPase of sarcoplasmic reticulum. *Biochim. Biophys. Acta* **1113**, 323-338.

Blasie, J. K., Herbette, L. G., Pascolini, D., Skita, V., Pierce, D. H. and Scarpa, A. (1985) Time-resolved X-ray diffraction studies of the sarcoplasmic reticulum membrane during active transport. *Biophys. J.* **48**, 9-18.

Carrington, A. and McLachlan, A. D. (1967) Introduction to magnetic resonance. Harper and Row, New York.

Cheong, G.-W., Young, H. S., Ogawa, H., Toyosima, C.and Stokes, D. L. (1996) Lamellar stacking in three-dimensional crystals of $Ca^{2+}$-ATPase from sarcoplasmic reticulum. *Biophys. J.* **70**, 1689-1699.

Cherry, R. J. (1979) Rotational and lateral diffusion of membrane proteins. *Biochim. Biophys. Acta* **559**, 289-327.

Cherry, R. J. and Godfrey, R. E. (1981) Anisotropic rotation of bacterorhodopsin in lipid membranes. *Biophys. J.* **36**, 257-276.

Clegg, R. M. and Vaz, W. L. C. (1985) Translational diffusion of proteins and lipids in artificial lipid bilayer membranes. A comparison of experiment with theory. *In* Progress in Protein-Lipid Interactions. Watts, A. and de Pont, J. J. H. H. M., editors.Vol. 1, Elsevier, Amsterdam, 173-229.

Dux, L. (1993) Muscle relaxation and sarcoplasmic reticulum function in different muscle types. *Rev. Physiol. Biochem. Pharmacol.* **122**, 2599-2603, Springer-Verlag, Berlin.

Dux, L. and Martonosi, A. (1983) $Ca^{2+}$-ATPase membrane crystals in sarcoplasmic reticulum. *J. Biol. Chem.* **258**, 10111-10115.

Dux, L. and Martonosi, A. N. (1983a) Two-dimensional arrays of proteins in sarcoplasmic reticulum and purified $Ca^{2+}$-ATPase vesicles treated with vanadate. *J. Biol. Chem.* **258**, 2599-2603.

Dux, L., Taylor, K. A., Ting-Beall, H. P. and Martonosi, A. N. (1985) Crystallization of the Ca-ATPase of sarcoplasmic reticulum by calcium and lanthanide ions. *J. Biol. Chem.* **260**, 11730-11743.

Eibl, H. and Lands, W. E. M. (1969) A new sensitive determination of phosphate. *Anal. Biochem.* **30**, 51-57.

Einstein, A. (1906) Eine neue Bestimmung der Molekuldimensionen. *Ann. Phys.* **19**, 379-388.

Esmann, M., Hideg, K.and Marsh, D. (1994) Influence of poly(ethylene glycol) and aqueous viscosity on the rotational diffusion of membranous Na,K-ATPase. *Biochemistry* **33**, 3693-3697.

Esmann, M., Horváth, L. I. and Marsh, D. (1987) Saturation transfer electron spin resonance studies on the mobility of spin-labeled sodium and potassium activated adenosinetriphosphatase in membranes from Squalus acanthias. *Biochemistry* **26**, 8675-8683.

Esmann, M., Sár, P. C., Hideg, K. and Marsh, D. (1993) Maleimide, iodoacetamide, indanedione, and chloromercuric spin label reagents with derivatized nitroxide rings as ESR reporter groups for protein conformation and dynamics. *Anal. Biochem.* **213**, 336-348.

Feynman, R. P., Leighton, R. B.and Sands, M. (1963) The Feynman lecture on physics. Chpt 20, Addison-Wesley Publishing Co., Inc. Reading, Massachusetts, USA.

Freed, J. H. (1976) Theory of slow tumbling ESR spectra for nitroxides. *In* Spin labeling. Theory and applications. Chpt. 3, Academic Press, New York.

Hankovszky, O. H., Hideg, K. and Jerkovich, Gy. (1989) Synthesis of 3-subtituted 2,5-dihydro-2,2,5,5-tetramethyl-1H pyrrol-1-yloxyl radicals Useful for spin labelling of biomolecules. *Synthesis* **52**, 526-529.

Hemminga, M. A., de Jager, P. A., Marsh, D.and Fajer, P. (1984) Standard conditions for the measurement of saturation transfer ESR spectra. *J. Magn. Reson.* **59**, 160-163.

Hidalgo, C. (1987) Lipid-protein interactions and the function of the $Ca^{2+}$-ATPase of Sarcoplasmic Reticulum. *CRC Crit.Rev. in Biochem.* **21**, 319-347.

Hidalgo, C. and Thomas, D. D. (1977) Heterogenity of SH groups in sarcoplasmic reticulum. *Biochem. Biophys. Res. Commun.* **78**, 1175-1182.

Horváth, L. I. and Marsh, D. (1983) Analysis of multicomponent saturation transfer ESR spectra using the integral method: application to membrane systems *J. Magn. Reson.* **54**, 363-373.

Horváth, L. I. and Marsh, D. (1988) Improved numerical evaluation of saturation transfer electron spin resonance spectra. *J. Magn. Reson.* **80**, 314-317.

Horváth, L. I., Dux, L., Hankovszky, H. O., Hideg, K. and Marsh, D. (1990) Saturation transfer electron spin resonance of $Ca^{2+}$ -ATPase covalently spin-labeled with β-substituted vinyl ketone- and maleimide-nitroxide derivatives. *Biophys. J.* **58**, 231-241.

Hyde, J. S. and Dalton, L. R. (1979) Saturation transfer spectroscopy. *In* Spin Labeling. Theory and Applications. Berliner, L. J., editor. Vol. 2, Academic Press, New York, 1-70.

Ingold, C. K. (1969) Structure and Mechanism in Organic Chemistry. 2nd ed., 1016-1023, Cornell Univ. Press, Ithaca, NY.

Jähnig, F. (1986) The shape of membrane protein derived from rotational diffusion. *Eur. J. Biophys.* **14**, 63-64.

Knowles, P. F. and Marsh, D. Magnetic resonance of membranes. (1991) *Biochem. J.* **274**, 625-641

Kramers, H. A. (1940) Brownian motion in a field of force and the diffusion model of chemical reactions. *Physica* **7**, 284-304.

Lewis, S. M. and Thomas, D. D. (1986) Effects of vanadate on the rotational dynamics of spin-labelled Ca-ATPase in sarcoplasmic reticulum membranes. *Biochemistry* **25**, 4615-4621.

Litovitz, T. A. (1952) Temperature Dependence of the viscosity of associated liquids. *J. Chem.Phys.* **20**, 1088-1089.

MacLennan, D. H. (1990) Molecular tools to elucidate problems in excitation-contraction coupling. *Biophys. J.* **58**, 1355-1365.

MacLennan, D. H., Brandl, C. J., Korczak, B. and Green, N. M. (1985) Amino-acid sequence of a $Ca^{2+}$+$Mg^{2+}$-dependent ATPase from rabbit muscle sarcoplasmic reticulum, deduced froom it complementary DNA sequence. *Nature* **316**, 696-700.

MacLennan, D. H., Clarke, D. M., Loo, T. W. and Skerjanc, I. S. (1992) Site-directed mutagenesis of the $Ca^{2+}$-ATPase of sarcoplasmic reticulum. *Acta. Physiol. Scand. Suppl.* **607**, 141-150.

Marsh, D. (1988) Molecular Mobility in Membranes. *In* Physical Properties of Biological Membranes and Their Functional Implications. Hidalgo, C., ed. Plenum Press, New York, 123-145.

Marsh, D. and Horváth, L. I. (1989) Spin label studies of the structure and dynamics of lipids and proteins in membranes. *In* Advanced EPR in Biology and Biochemistry. Hoff, A. J., Elsevier Publisher, Amsterdam, 707-772.

Marsh, D. and Horváth, L. I. (1992) A simple analytical treatment of the sensitivity of saturation transfer EPR spectra to slow rotational diffusion. *J. Magn. Reson.* **99**, 323-331.

Martonosi, A. (1984) Mechanism of $Ca^{2+}$ release from sarcoplasmic reticulum of skeletal muscle. *Physiol. Rev.* **64**, 1240.

Martonosi, A. (1992) The $Ca^{2+}$-transport ATPases of sarco(endo)-plasmic reticulum and plasma membranes. *In* Molecular Aspects of Transport Proteins, Ed. De Pont, J. J. H. H. M., New comprehensive Biochemistry. Vol. 21, Elsevier Science Publishers B. V., 57-114.

Martonosi, A. N. and Beeler, T. J. (1983) *In* Handbook of Physiology, Skeletal Muscle. Peachey, L. D., Adrian, R. H. and Geiger, S. R., eds., American Physiological Society, Bethesda, 417-485.

Nakamura, H., Jilka, R. L., Boland, R. and Martonosi, A. N. (1976) Mechanism of ATP hydrolysis by sarcoplasmic reticulum and the role of phospholipids. *J. Biol. Chem.* **251**, 5414-5423.

Napier, R. M., East, J. M. and Lee, A. G. (1987) State of aggregation of the (Ca+Mg)-ATPase studied using saturation-transfer electron spin resonance. *Biochim. Biophys. Acta* **903**, 365-375.

Napolitano, C. A., Cooke, P., Segalman, K. and Herbette, L. (1983) Organization of calcium pump protein dimers in the isolated SR membrane. *Biophys. J.* **42**, 119-125.

Ohnishi, S. and McConnell, H. (1965) *J. Am. Chem. Soc.* **87**, 2293.

Robinson, B. H. and Dalton, L. R. (1980) Anisotropic rotational duffusion studied by passage saturation transfer electron paramagnetic resonance. *J. Chem. Phys.* **72**, 1312-1324.

Roopnarine, O., Hideg, K. and Thomas, D. D. (1993) Saturation transfer electron paramagnetic resonance of indane-dione spin-label. *Biophys. J.* **64**, 1896-1907.

Rozantsev, E. G., and Sholle, V. D. (1971) Synthesis and reactions of stable nitroxyl radicals. I. Synthesis. *Synthesis*, 190-202.

Saffman, P. G. and Delbrück, M. (1975) Brownian motion in biological membranes. *Proc. Natl. Acad. Sci. USA* **72**, 3111-3113.

Sandermann, H. (1978) Regulation of membrane enzymes by lipids. *Biochim. Biophys. Acta* **515**, 209-237.

Schreier, S., Polnaszek, C. F. and Smith, I. C. P. (1978) Spin labels in membranes. Problems in practice. *Biochim. Biophys. Acta* **515**, 375-436.

Shi, D., Hsiung, H.-H., Pace, R. C. and Stokes, D. L. (1995) Preparation and analysis of large, flat crystals of $Ca^{2+}$-ATPase for electron crystallography. *Biophys. J.* **68**, 1152-1162.

Smith, I. C. P. (1972) The spin label method *In* Biological applications of electron spin resonance. Swartz H. M., Bolton J. R., Borg, D. C., eds. 483-541 , Wiley-Interscience, USA.

Sousa, R. (1995) Use of Glycerol, Polyols and Other Protein Structure Stabilizing Agents in Protein Crystallization *Acta Cryst.* **D51**, 271-277.

Squier, T. C. and Thomas, D. D. (1986) Methodology for increased precision in saturation transfer electron paramagnetic resonance studies of rotational dynamics *Biophys. J.* **49**, 921-935.

Squier, T. C., Hughes, S. E. and Thomas, D. D. (1988) Rotational dynamics and protein-protein interactions in the Ca-ATPase mechanism *J. Biol. Chem.* **263**, 9162-9170.

Stone, T., Buckman, T., Nordio, P. and McConnell, H. M. (1965) Spin-labeled biomolecules. *Proc. Natl. Acad. Sci.* 54, 1010.

Taylor, K. A., Dux, L. and Martonosi, A. (1986) Three-dimensional reconstruction of negatively stained crystals of the $Ca^{2+}$-ATPase from muscle sarcoplasmic reticulum. *J. Mol. Biol.* **187**, 417-427.

Taylor, K. A., Ho, M. H. and Martonosi, A. (1986) Image analysis from the $Ca^{2+}$-ATPase from sarcoplasmic reticulum. *Ann. Rev. NY Acad. Sci.* **483**, 31-43.

Thomas, D. D., Dalton, L. R. and Hyde, J. S. (1976) Rotational diffusion studied by passage saturation transfer electron paramagnetic resonance. *J. Chem. Phys.* **65**, 3006-3024.

Toyoshima, Ch., Sasabe, H. and Stokes, D. L. (1993) Three-dimensional cryo-electron microscopy of the calcium ion pump in the sarcoplasmic reticulum membrane. *Nature* **362**, 469-471.

Varga, S., Mullner, N., Pikula, S., Papp, S., Varga, K. and Martonosi, A. (1986) Pressure effects on sarcoplasmic reticulum.. *J. Biol. Chem.* **261**, 13943-1396.

Varga, S., Taylor, K. A. and Martonosi, A. (1991) Effect of solutes on the formation of crystalline sheets of the $Ca^{2+}$-ATPase in detergent-solubilized sarcoplasmic reticulum. *Biochim. Biophys. Acta* **1070**, 374-386.

Watts, A. and de Pont, J. J. H. H. M. (1985) Protein-lipid interactions. Vol. I, Elsevier Science, Amsterdam.